Supporting Information

Well-Defined Hierarchical Teddy Bear Sunflower-Like $NiCo_2O_4$ electrocatalyst for Superior Water Oxidation

Pradnya M. Bodhankar,[a,b] Dattatray S. Dhawale,*[c] Sarbjit Giddey,[c] Ravi Kumar,[d,e] and Pradip B. Sarawade,*[a,b]

[a]*National Centre for Nanosciences and Nanotechnology, University of Mumbai, Kalina, Mumbai-400098, India.*

[b]*Department of Physics, University of Mumbai, Kalina, Mumbai-400098, India.*

[C]*CSIRO Energy, Private Bag 10, Victoria, Clayton South 3169, Australia.*

[d] *Academy of Scientific and Innovative Research, CSIR-Human Resource Development Center (CSIR-HRDC) Campus, Postal Staff College Area, Ghaziabad, Uttar Pradesh, 201002, India*

[e] *Electronic Structure Theory Group, Physical and Materials Chemistry Division, CSIR-National Chemical Laboratory, Pune, 411008, India*

Corresponding Author

*E-mail: dattatray.dhawale@csiro.au, pradipsarawade@yahoo.co.in

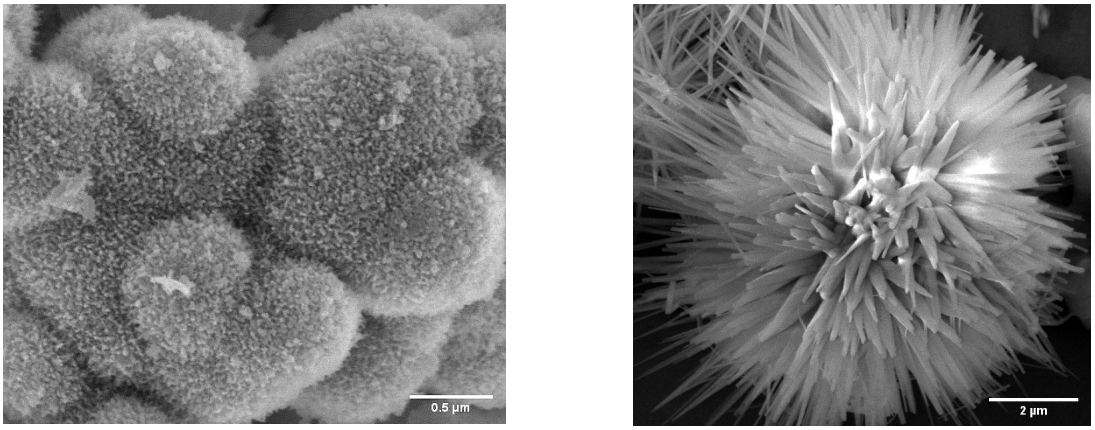

NiO Co_3O_4

Fig. S1. FE-SEM images of NiO and Co_3O_4 samples.

Table S1. Lattice parameters extracted from XRD data.

Sample	Lattice constant (Å)	The average crystallite size (nm)
$NiCo_2O_4$	8.102	5.4
NiO	4.177	18.5
Co_3O_4	8.075	14.8

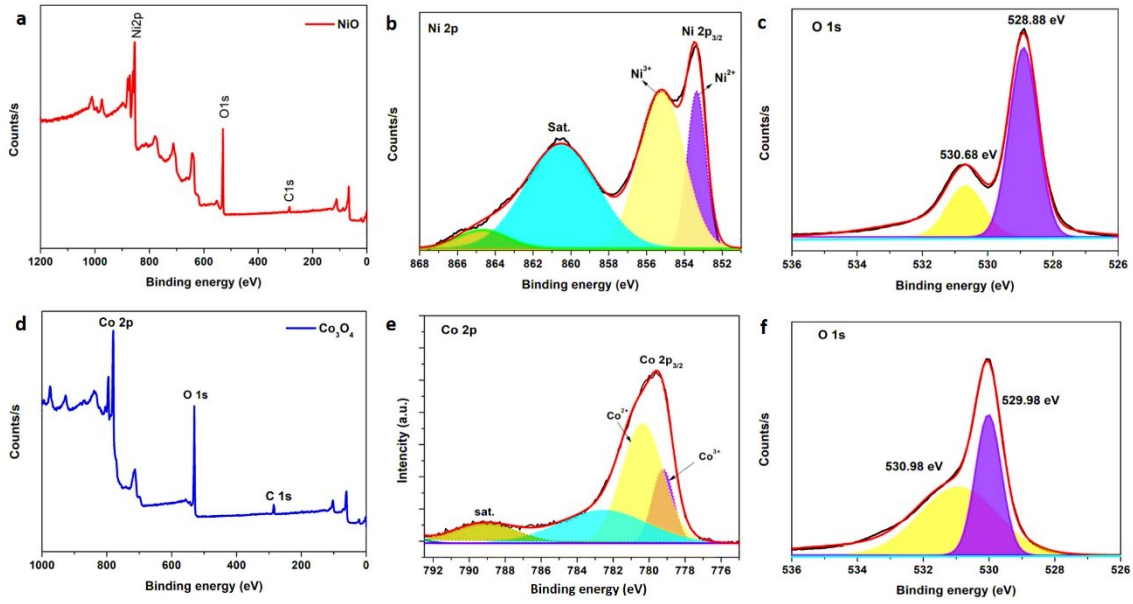

Fig. S2. XPS survey scan (a), High-resolution XPS spectra for Ni 2p (b), and O 1s states in NiO (c). XPS survey scan (d), High-resolution XPS spectra for Co 2p (b), and O 1s state in Co_3O_4.

Table S2. X-ray photoelectron spectra analysis data of the prepared samples.

Sample	Ni $2p_{3/2}$ Position (eV)		Co $2p_{3/2}$ Position (eV)		O 1s Position (eV)	
	Ni^{2+}	Ni^{3+}	Co^{2+}	Co^{3+}	O_I	O_{II}
$NiCo_2O_4$	853.78	855.58	779.38	780.68	529.28	531.00
NiO	853.48	855.28	-	-	528.88	530.68
Co_3O_4	-	-	780.88	779.78	529.98	530.98

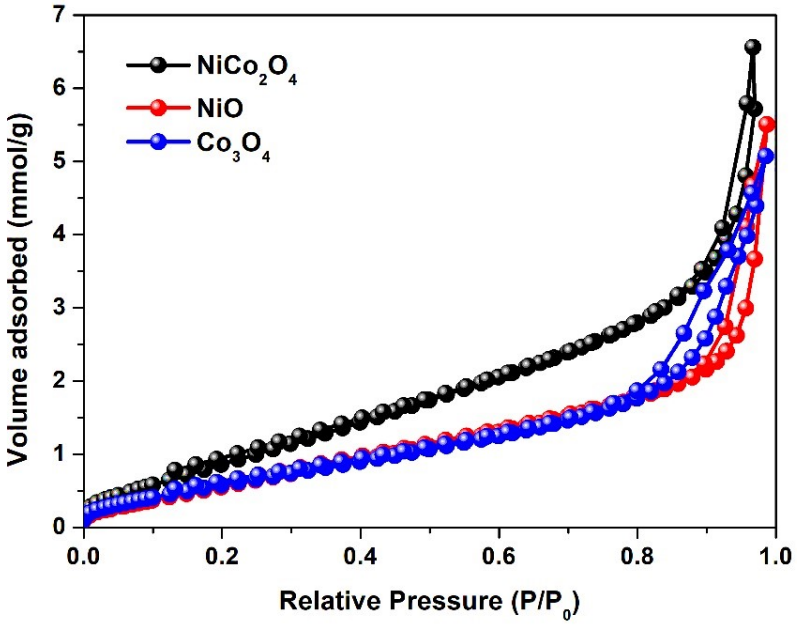

Fig. S3. N_2 Adsorption-desorption isotherm of obtained from BET measurements for $NiCo_2O_4$, NiO, and Co_3O_4 samples.

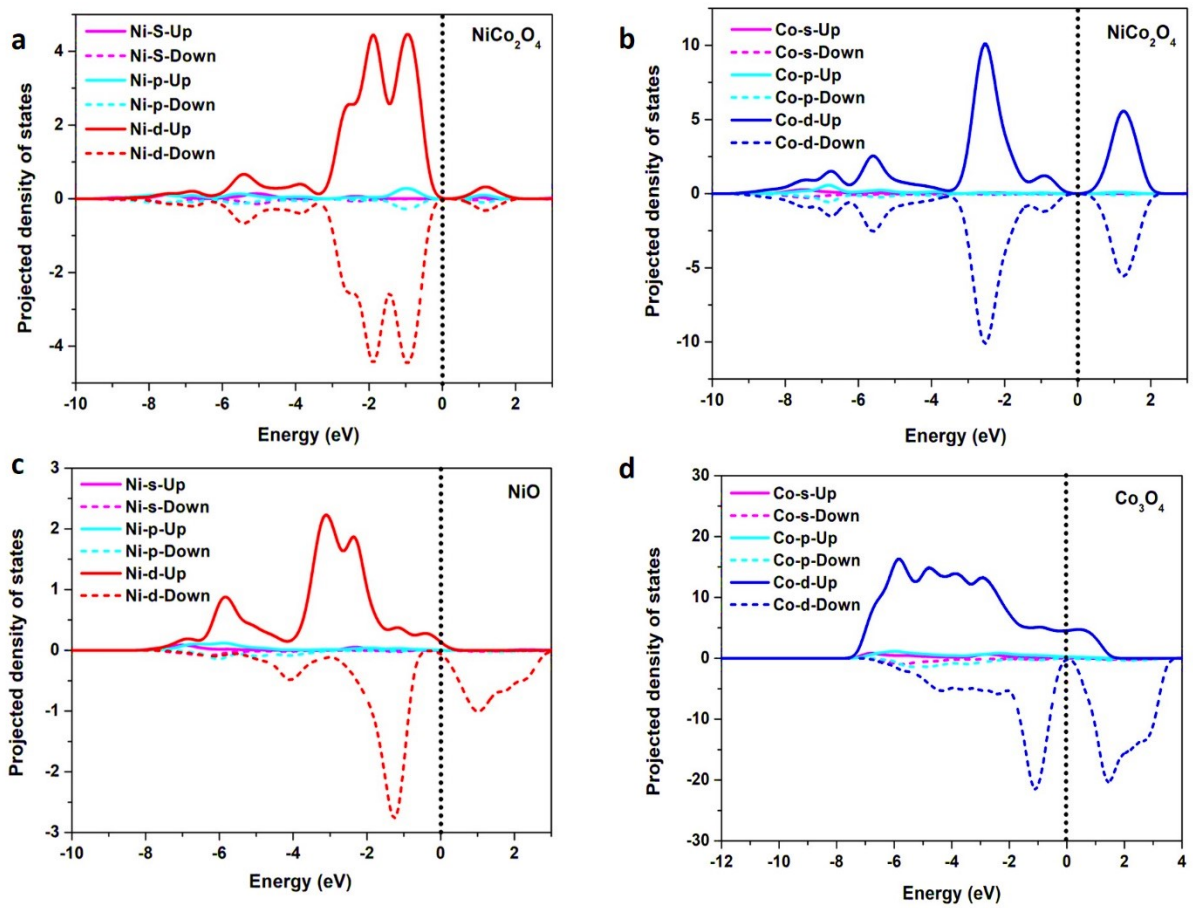

Fig. S4. The projected density of states for Ni (a) and Co (b) in $NiCo_2O_4$, respectively; Ni in NiO (c) and Co in Co_3O_4 (d). The spin-up PDOS are shown on a positive scale (solid line), while spin-down PDOS are shown on a negative scale (dashed line). The Fermi level is aligned to 0 eV.

The electronic occupancy in the d-orbital is calculated using the following formula[1]:

$$d\ orbital\ occupancy = \frac{DOS\ area\ below\ Fermi\ level}{Total\ DOS\ area} \quad \text{-------- (1)}$$

Table S3. The electronic d-orbital occupancy in $NiCo_2O_4$, NiO, and Co_3O_4 materials.

Catalyst	Atom	Spin	d orbital occupancy (%)
$NiCo_2O_4$	Ni	Up	96
		Down	96
	Co	Up	75
		Down	75
NiO	Ni	Up	93
		Down	51
Co_3O_4	Co	Up	98
		Down	66

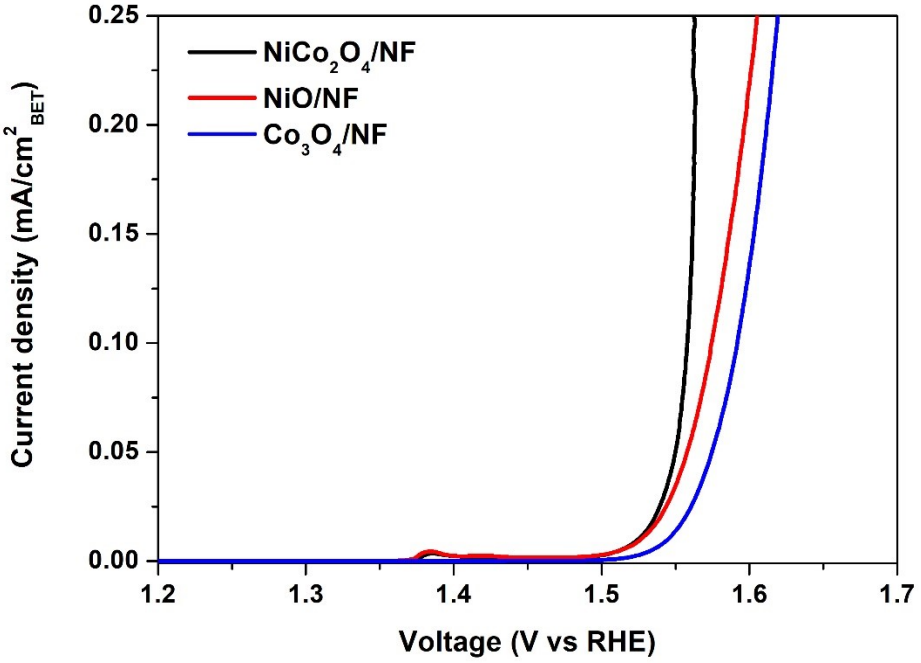

Fig. S5. BET surface area normalized linear polarization curves at a scan rate of 1 mV/s $NiCo_2O_4$/NF, NiO/NF, Co_3O_4/NF catalysts for OER.

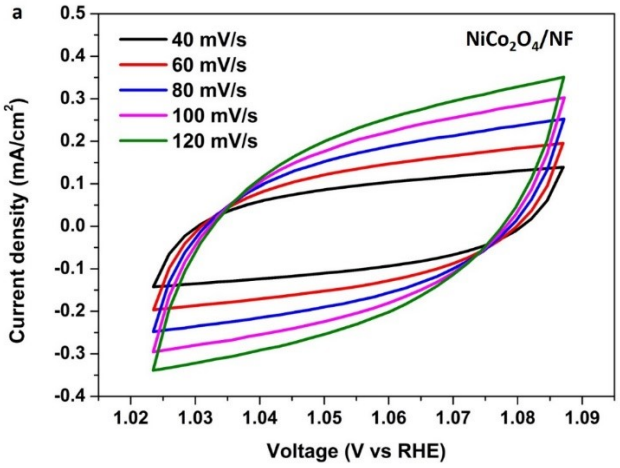

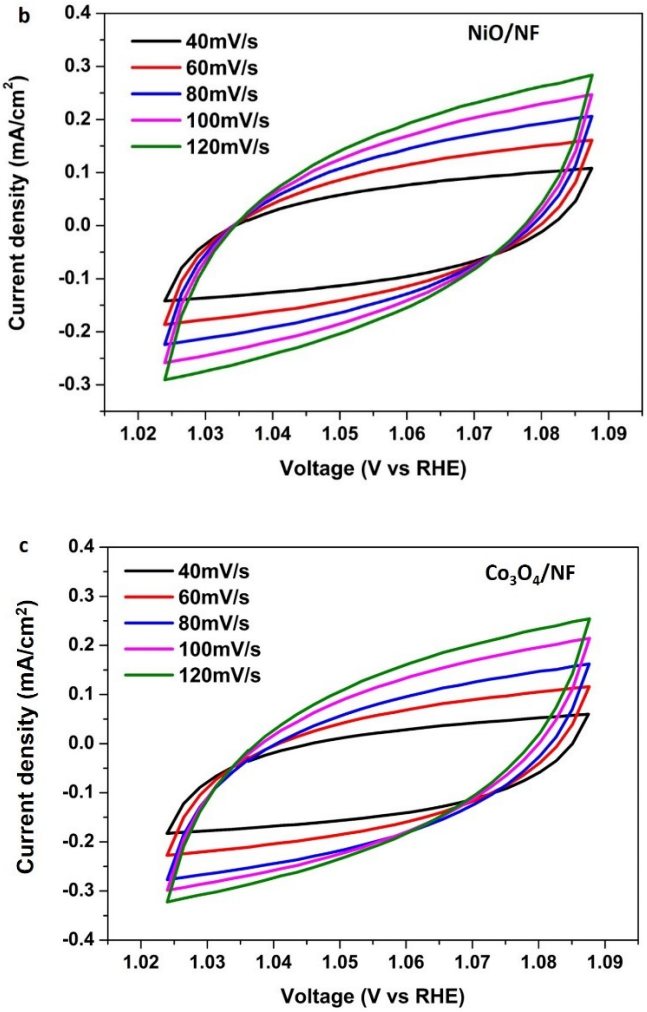

Fig. S6. CV curves at various scan rates to determine the double-layer capacitance (C_{dl}) of $NiCo_2O_4$/NF, NiO/NF, and Co_3O_4/NF catalysts.

Table S4. Solution resistance (R_s), Charge transfer resistance (R_{ct}), and double layer capacitance values of $NiCo_2O_4$/NF, NiO/NF, and Co_3O_4/NF catalysts.

Catalyst	R_s (Ω cm^2)	R_{ct} (Ω cm^2)	C_{dl} (mF/cm^2)
$NiCo_2O_4$/NF	1.00	1.15	1.68
NiO/NF	1.00	2.44	1.07
Co_3O_4/NF	1.00	3.67	0.69

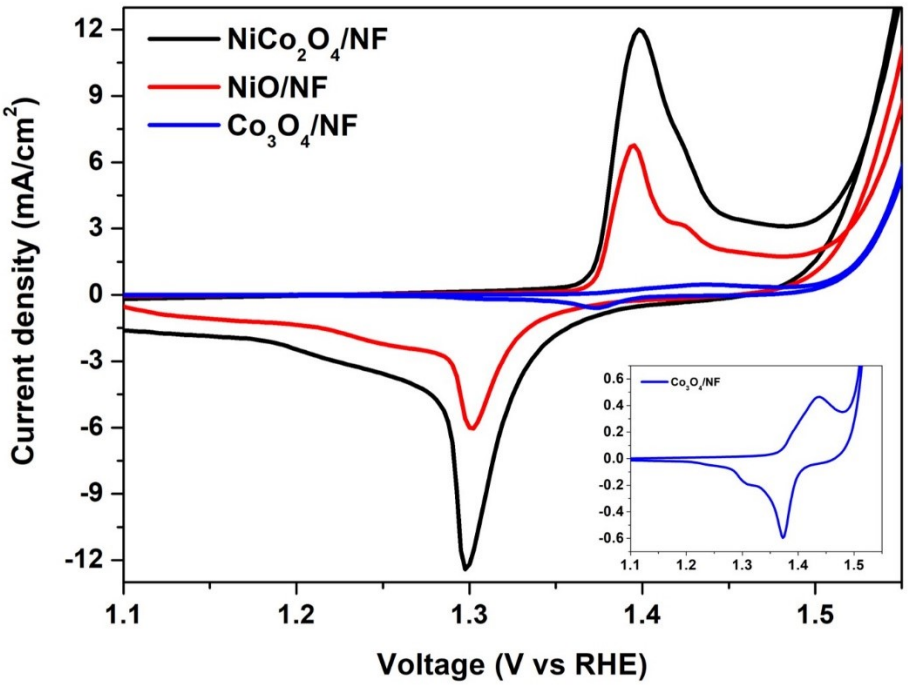

Fig. S7. Cyclic voltammetry scan for $NiCo_2O_4$/NF, NiO/NF, and Co_3O_4/NF catalysts at a scan rate of 2 mV/s in 1 M KOH.

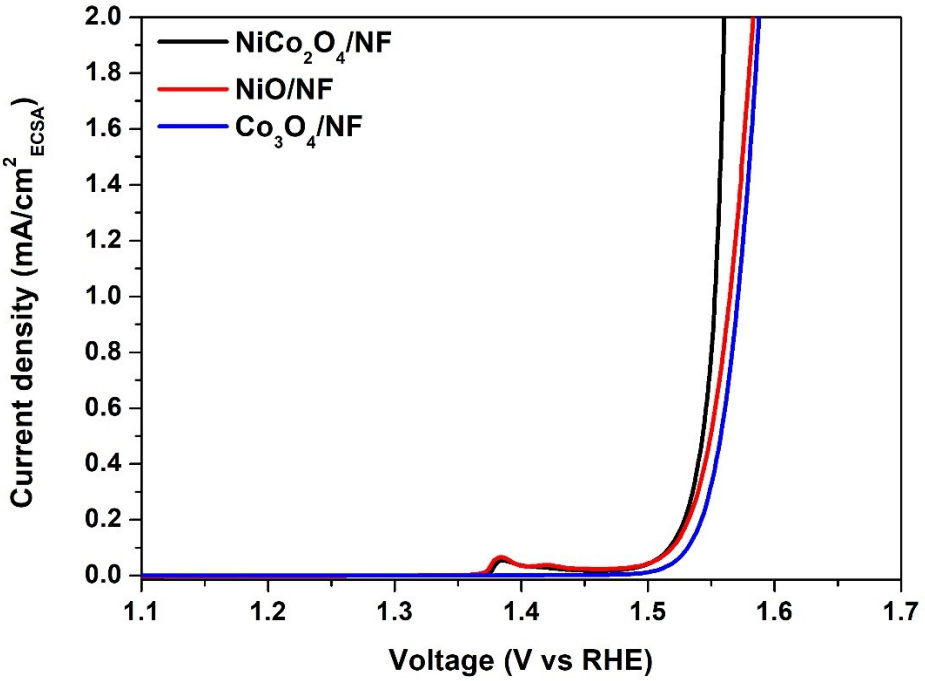

Fig. S8. ECSA-corrected LSV curves for $NiCo_2O_4$/NF, NiO/NF, and Co_3O_4/NF catalysts.

Catalyst utilization (%): $\frac{ECSA\ (m^2/gm)}{BET(m^2/gm)} \times 100$ ---------- (2)

Table S5. Catalyst utilization of $NiCo_2O_4$/NF, NiO/NF, and Co_3O_4/NF catalysts.

Catalyst	Utilization (%)
$NiCo_2O_4$/NF	64.28
NiO/NF	62.45
Co_3O_4/NF	42.75

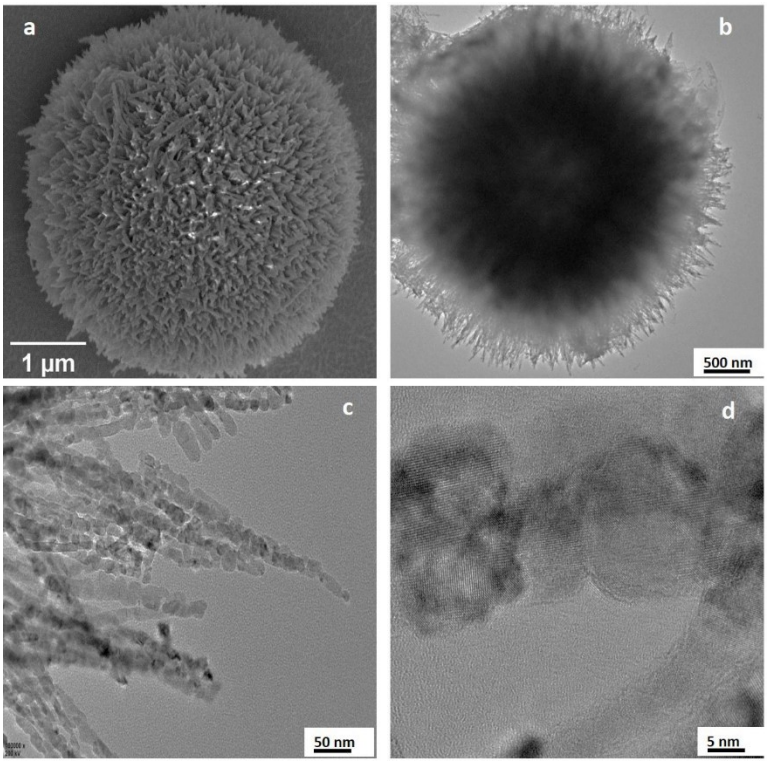

Fig. S9. Post-OER SEM (a), low and high magnification TEM images (b-d) of $NiCo_2O_4$/NF catalyst.

Table S6. Comparison of recent Ni-based electrocatalysts for OER active in alkaline media.

Catalyst	Morphology	Electrolyte	Over-potential (mV) at 10 mA/cm^2	Tafel slope (mV/dec)	Stability (hours)	Ref.
$NiCo_2O_4$/NF	**Teddy bear sunflower-like**	**1 M KOH**	**290**	**37**	**16**	**This work**
NiO/NF	**Spherical**	**1 M KOH**	**300**	**48**	**-**	**This work**
Co_3O_4/NF	**Sea-urchin**	**1 M KOH**	**322**	**54**	**-**	**This work**
$NiCo_2O_4$	Nanosheets	1 M KOH	290	91	14	[2]
$CoMn_2O_4$/rGO	Nanorods	0.1 MKOH	310	56	-	[3]
$NiCo_2O_4$/GF	Nanoflakes	1 M KOH	300	61	40	[4]
$NiCo_2O_4$@ NiMoO4	Core–Shell Hybrid Nanorods	1 M KOH	250	58.7	12	[5]
$NiCo_2O_4$@ C	Urchin-like peapod	1 M NaOH	267	46.5	30	[6]
Ni@$NiCo_2O_4$	Hollow core-shell nanorod array	1 M KOH	270	67	40	[7]
$NiCo_2O_4$	Hollow micro-cuboids	1 M NaOH	290	53	32	[8]
Ar-$NiCo_2O_4$|S	Nanosheet arrays	1 M KOH	256	51.1	24	[9]
$NiCo_2O_4$@ Ni_2P	Nanorods	1 M KOH	350	59	6	[10]

$NiCo_2O_4$@Ni WO_4/NF	Nanorod arrays	1 M KOH	310	102.8	12	[11]
$NiCo_2O_4$@ MnOx	Core-shell nanowires	0.1 M KOH	342	64	100	[12]
N-$NiCo_2O_4$@ C@NF	Nanowires	1 M KOH	242	65	25	[13]
$NiCo_2O_4$/Ti	Nanosheets	1 M KOH	353	61	20	[14]
$NiCo_2O_4$/NiO	Nanosheets	1 M NaOH	360	61	11	[15]
FeNiP@N-CFs	Nanoparticles	1 M KOH	300	47	20	[16]

References

1. T.-C. Chang, Y.-T. Lu, C.-H. Lee, J. K. Gupta, L. J. Hardwick, C.-C. Hu and H.-Y. T. Chen, *ACS omega*, 2021, **6**, 9692-9699.
2. R. Zhao, D. Cui, J. Dai, J. Xiang and F. Wu, *Sustainable Materials and Technologies*, 2020, **24**, e00151.
3. J. Du, C. Chen, F. Cheng and J. Chen, *Inorganic Chemistry*, 2015, **54**, 5467-5474.
4. Z. Liu, H. Tan, D. Liu, X. Liu, J. Xin, J. Xie, M. Zhao, L. Song, L. Dai and H. Liu, *Advanced Science*, 2019, **6**, 1801829.
5. X. Du, J. Fu and X. Zhang, *ChemCatChem*, 2018, **10**, 5533-5540.
6. J. Deng, H. Zhang, Y. Zhang, P. Luo, L. Liu and Y. Wang, *Journal of Power Sources*, 2017, **372**, 46-53.
7. L. Wang, C. Gu, X. Ge, J. Zhang, H. Zhu and J. Tu, *ChemNanoMat*, 2018, **4**, 124-131.
8. X. Gao, H. Zhang, Q. Li, X. Yu, Z. Hong, X. Zhang, C. Liang and Z. Lin, *Angewandte Chemie International Edition*, 2016, **55**, 6290-6294.
9. J. H. Lin, Y. T. Yan, T. X. Xu, C. Q. Qu, J. Li, J. Cao, J. C. Feng and J. L. Qi, *Journal of Colloid and Interface Science*, 2020, **560**, 34-39.
10. Q. Wang, H. Wang, X. Cheng, M. Fritz, D. Wang, H. Li, A. Bund, G. Chen and P. Schaaf, *Materials Today Energy*, 2020, **17**, 100490.
11. X. Du, Q. Shao and X. Zhang, *International Journal of Hydrogen Energy*, 2019, **44**, 2883-2888.
12. L. Zeng, T. Zhao, R. Zhang and J. Xu, *Electrochemistry Communications*, 2018, **87**, 66-70.
13. Y. Ha, L. Shi, X. Yan, Z. Chen, Y. Li, W. Xu and R. Wu, *ACS Applied Materials & Interfaces*, 2019, **11**, 45546-45553.
14. W. Bao, L. Xiao, J. Zhang, P. Jiang, X. Zou, C. Yang, X. Hao and T. Ai, *International Journal of Hydrogen Energy*, 2021, **46**, 10259-10267.
15. C. Mahala and M. Basu, *ACS omega*, 2017, **2**, 7559-7567.
16. R. Mo, S. Wang, H. Li, J. Li, S. Yang and J. Zhong, *Electrochimica Acta*, 2018, **290**, 649-656.